Digital Assessment of Initial Geometric Imperfections in Full-Scale 3D Concrete Printed Walls Using Terrestrial Laser Scanning and Eurocode 2 Evaluation

Jun Liang Ben Ng [1], Wei Liang, Ivan Seng [2], J Y Richard Liew [3], Meiling Dai [4], Hongjian Du [5]

[1,2,3,4,5] National University of Singapore, Department of Civil and Environmental Engineering, Singapore
[1] ngjunliangben01@u.nus.edu, [2] ivan.seng@u.nus.edu, [3] ceeljy@nus.edu.sg, [4] daimeiling@nus.edu.sg, [5] ceedhj@nus.edu.sg,

Abstract

Eurocode 2 (EC2) requires second-order effects to be considered for slender concrete members because small initial geometric imperfections can amplify bending moments and reduce load capacity. For 3D concrete printing (3DCP), such imperfections are strongly process-dependent (e.g., printhead path accuracy, calibration drift, and environmental effects), making it uncertain whether conventional EC2 imperfection assumptions remain conservative. This paper condenses a digital workflow that uses terrestrial laser scanning (TLS) point clouds to quantify as-built geometric imperfections of full-scale 3DCP walls. The point cloud is cleaned, sliced at millimetre resolution, and converted into cross-sectional descriptors (area and centroid) along wall height after a consistent principal component analysis (PCA) -based alignment. The measured imperfection profile is then benchmarked against EC2 serviceability (inclination) and ultimate (equivalent eccentricity) limits. Three full-scale walls (200 mm × 1000 mm × 3000 mm design size) were scanned and assessed. All walls remained within the conservative envelope. The study demonstrates how scan-derived imperfection metrics can be used to support objective quality control and code-based structural assessment of 3DCP walls.

Keywords –

3D concrete printing; terrestrial laser scanning; point cloud; centroid drift; geometric imperfection; Eurocode 2; quality control

1 Introduction

3D concrete printing (3DCP) has emerged as a construction automation approach that deposits cementitious material layer-by-layer along a digital toolpath. The layer-wise deposition eliminates formwork but also means the as-built geometry is strongly governed by printer kinematics, nozzle calibration, extrusion stability, material rheology, and environmental conditions during printing. Printed walls therefore often show geometric signatures that differ from conventional tolerances, including layer-to-layer offsets, surface waviness, and gradual departures from verticality or rotation relative to a nominal centreline (Figure 1). In Figure 1, ‘a’ and ‘b’ refers to the resulting horizontal layer offsets from the nominal centreline while ‘c’ refers to the greatest horizontal layer offset from the nominal centreline due to a global tilting of the print layers. These deviations are inherently linked to the production process, and warrant objective, repeatable quality assessment methods rather than purely visual inspection [1].

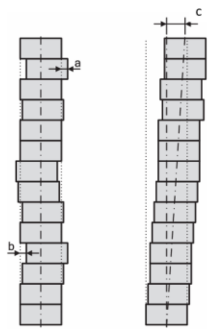

Figure 1: Displacement between layers (left) and angular deviation of the wall with respect to the nominal centreline (right). Reproduced from [1]

For slender wall members, geometric deviations are not only manufacturing-quality issues; they can become initial imperfections that introduce unintended eccentricity, amplify second-order effects, and affect structural stability [2]. In reinforced concrete design, Eurocode 2 (EC2) accounts for such behaviour using simplified imperfection models [3]. For isolated members, EC2 provides checks based on a global inclination limit at the serviceability limit state and an equivalent eccentricity allowance at the ultimate limit state. However, these EC2 assumptions were developed primarily for conventionally constructed members and may not reflect process-driven, spatially varying imperfection patterns produced by 3DCP. In practice, this creates uncertainty over whether code-based limits can be applied directly, or whether measured imperfections should be used to avoid unconservative assessments.

Terrestrial laser scanning (TLS) and related 3D scanning technologies now enable dense, millimetre-scale point clouds of as-built surfaces, making it feasible to measure deviations directly rather than infer them from assumed tolerances. In parallel with the digitalisation of 3DCP, scanning and monitoring are increasingly incorporated into larger digital workflows for on-site printing and quality control [4], [5]. At the specimen scale, scan data have been used to reconstruct "as-built" digital models of printed walls for geometric evaluation and downstream engineering tasks, informing design and simulation workflows [4] . Processing the laser scan can further support wall-height profiling of geometric characteristics, such as thickness-related measures and cross-sectional descriptors (e.g., area and centroid) [4], [5], [6]. However, converting raw scans into stable engineering metrics is non-trivial: point clouds contain noise and occlusions, registration choices can introduce bias, and a consistent reference frame is required so that slice-by-slice comparisons represent true geometric drift.

Despite this progress, many scan-based assessments remain oriented toward dimensional conformity and surface quality, and fewer translate point-cloud measurements into structural imperfection descriptors that map directly to code checks for slender members. To the authors' knowledge, no existing study has presented a complete workflow that converts TLS point clouds of 3DCP walls into cross-sectional centroid drift profiles and directly benchmarks them against Eurocode 2 imperfection limits for isolated slender members. While prior work has used scan data for dimensional conformity and surface quality assessment [4], [5], [6], the translation of scan-derived geometry into code-relevant structural imperfection descriptors — specifically inclination and equivalent eccentricity — has not been systematically addressed for 3DCP elements. This paper addresses that gap by developing a practical, repeatable scan-to-metrics workflow that (i) quantifies cross-sectional area variation and centroid drift along wall height from TLS point clouds, and (ii) benchmarks the resulting imperfection profile against EC2 criteria for isolated slender members.

2 3D printing and scanning of wall specimens

Three full-scale 3DCP walls (Figure 2) were printed and scanned under realistic fabrication conditions. The nominal CAD dimensions were 200 mm (thickness) × 1000 mm (length) × 3000 mm (height), corresponding to a nominal cross-sectional area of 200,000 mm². All walls were scanned with the FARO Focus M 70 (Figure 3) at 7-8 sides (Figure 4) and processed using the same slicing interval and alignment strategy to enable consistent comparison.

Figure 2: Printing of 3DCP walls

Figure 3: Photo of FARO Focus M70 Laser Scanner

Figure 4: 3D scans acquired at 7 to 8 sides around 3DCP wall

3 Methodology

The proposed workflow in Figure 5 converts raw TLS point clouds into imperfection metrics that are directly interpretable in structural design checks. The main stages are: (1) TLS data acquisition and registration, (2) point-cloud preprocessing, (3) horizontal slicing and cross-section reconstruction, (4) coordinate normalisation and alignment, and (5) imperfection metric extraction and EC2 benchmarking.

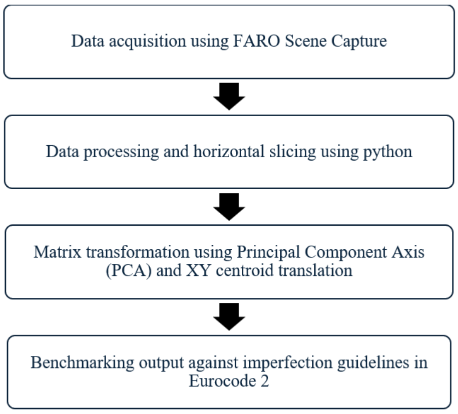

Figure 5: Workflow of Point Cloud Data Processing

3.1 Data acquisition and registration

Full-scale 3DCP wall specimens were scanned using a FARO Focus terrestrial laser scanner. Multiple scans were taken around each wall to reduce occlusion. Prior to scanning, calibration was performed using a checkerboard target (Figure 6) to confirm measurement accuracy within the manufacturer tolerance of ± 1mm.

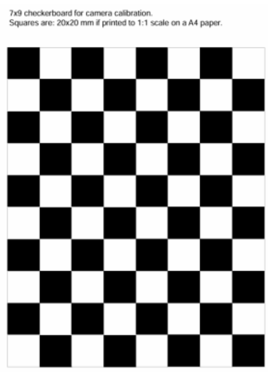

Figure 6: Checkerboard for calibration

Scans were registered in FARO Scene with a two-point level-preserving alignment approach, cropped to isolate the wall geometry, and exported as XYZ point clouds for downstream processing.

3.2 Point-cloud preprocessing

Statistical Outlier Removal (SOR) was first applied to suppress isolated noise points while preserving the wall surface, using a conservative standard deviation threshold to avoid removing valid geometric features. Environmental noise was removed using SOR implemented in the Open3D library. The SOR algorithm operates by evaluating the mean distance of each point to its nearest neighbors and comparing these distances to the overall distribution within the dataset. Points that deviate significantly from this distribution are classified as outliers and removed. This process reduces random scatter while retaining the shape of the scanned geometry.

The algorithm uses two user-defined parameters which are “nb_neighbors” and “std_ratio”. The first parameter “nb_neighbors” specifies the number of neighboring points to be considered when calculating the local mean distance around an arbitrary point in the cloud. The second parameter “std_ratio” refers to the standard deviation multiplier that determines the threshold for outlier removal. Lower “std_ratio” values result in more aggressive filtering, whereas higher values remove only the most extreme points.

The Open3D documentation illustrates the use of these parameters with sample values of “nb_neighbors” = 20 and “std_ratio” = 2.0 [7]. For this study, “nb_neighbors” was set to 20 and “std_ratio” to 4.0. This conservative configuration was selected to eliminate only the most significant outliers, thereby minimizing the risk of discarding valid geometric information from the wall surface. A sample of how the output of the SOR algorithm can be seen in Figure 7 where the noise is found to be an outlier and removed.

Figure 7: Outlier removal using statistical outlier removal (SOR) algorithm

3.3 Horizontal slicing and cross-section descriptors

The cleaned point cloud was partitioned into horizontal slices at 1 mm intervals. To avoid artefacts near the base and top (e.g., fixtures, termination effects, partial layers) as seen in Figure 8, only a stable region was analysed by excluding approximately one layer thickness from both ends. For each slice, the XY boundary was reconstructed and used to compute (i) cross-sectional area and (ii) slice centroid. For the near-rectangular wall cross-sections studied, convex hull boundaries produced areas comparable to more complex concave-hull approaches and were adopted for computational robustness.

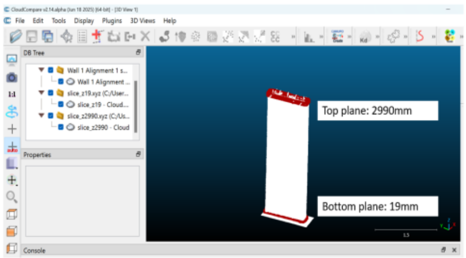

Figure 8: Visualisation of bottom and top plane in CloudCompare

3.4 Alignment and coordinate normalisation

Because scan coordinates depend on scanner setup and registration reference, a consistent local coordinate system was enforced (Figure 10). A reference slice near the base was used to define orientation via principal component analysis (PCA): the dominant PCA direction was aligned with the global wall axis, and the centroid of the reference slice was translated to the origin. The same rotation–translation transform was then applied to all slices to obtain a consistent centroid drift profile along height.

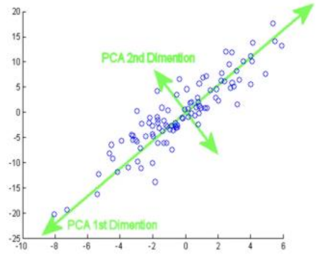

Figure 9: Illustration of Principal Component Analysis, reproduced from [8]

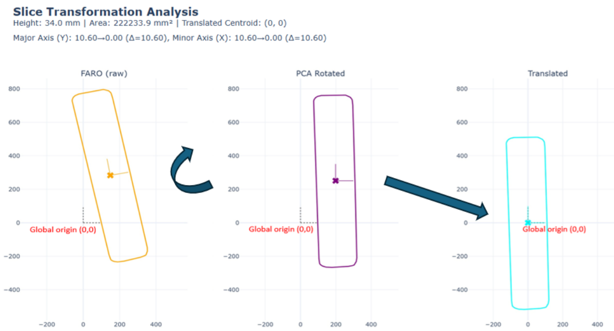

Figure 10: Illustration of PCA rotation and XY translation of FARO scan

3.5 Imperfection metrics and Eurocode 2 benchmarking

The imperfection profile was expressed through two EC2-aligned descriptors, via an inclination θ_1 (Clause 5.2 (5)) and as an eccentricity e_i (Clause 5.2 (7)). First, global inclination was obtained from the ratio of maximum lateral centroid offset to the analysed height and compared with the EC2 inclination limit (0.005 rad) as stated in clause 5.2 (5). Second, an equivalent geometric eccentricity was evaluated from the centroid offset and compared with the EC2 ultimate-limit imperfection allowance for isolated members. For isolated members, the maximum allowable eccentricity, e_i is defined as $L_0/400$ where L_0 denotes the effective length of the member. For the wall height of 3000 mm, the corresponding EC2 eccentricity limit was approximately 7.5 mm. In this case, the out of plumbness is considered as the eccentricity, e_i.

$$\theta_1 \text{ (radian)} = tan^{-1} \left(\frac{out\ of\ plumbness, e_i}{vertical\ height, Z}\right) \quad (1)$$

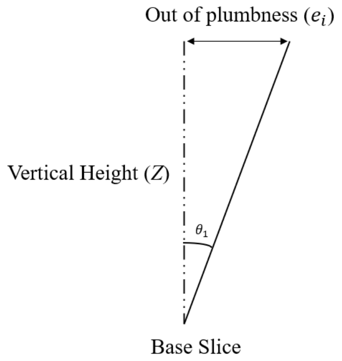

Figure 11: Illustration of out of plumbness with respect to the base slice

Wall	Cross section area (mm^2)	Max eccentricity (mm)	Max inclination (rad)
1	218622±3394	5.60	0.0018
2	221535±3457	3.13	0.0010
3	219525±4898	2.81	0.0009

Table 1. Summary of scan-derived imperfection metrics and EC2 checks.

4 Results

The results of the minor axis eccentricity for the three full scale specimens (W1, W2, W3), are plotted in Figure 12. Table 1 summarises the key imperfection metrics derived from the TLS point clouds. All walls showed minor drift and remained within EC2 limits. Across all three walls, the measured cross-sectional areas generally exceeded the nominal CAD area of 200000 (mm^2), indicating overprinting under the selected printing conditions.

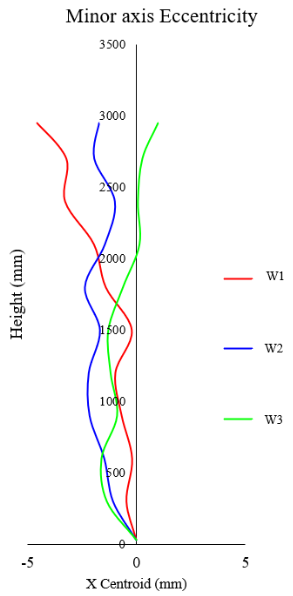

Figure 12: Minor axis eccentricity of 3DCP walls

5 Discussion

The results from three nominally similar full-scale walls highlight a key characteristic of 3DCP: geometric imperfection is not only a function of the intended CAD geometry, but also of process stability and calibration during printing. Using the proposed scan-to-metrics workflow, all specimens exhibited only minor centroid drift along height and remained within the EC2 inclination and equivalent eccentricity limits adopted for isolated slender members. For the printing conditions represented in this dataset, this suggests that EC2's simplified imperfection assumptions provide a conservative envelope for global inclination and geometric eccentricity, and that the walls satisfy code-consistent imperfection checks when assessed using measured as-built geometry.

While independent reference measurements (e.g., total station or manual plumb-bob surveys) were not available for cross-validation in this study, the measurement uncertainty is bounded by the scanner's verified accuracy of ± 1 mm, confirmed through checkerboard calibration prior to each scan session. The largest measured eccentricity (5.60 mm for Wall 1) is well above this instrument uncertainty, and the EC2 eccentricity limit of 7.5 mm provides additional margin. Furthermore, the consistency of the cross-sectional area measurements — all three walls independently showed areas approximately 10% above the nominal CAD value, consistent with known overprinting behaviour — supports the reliability of the processing pipeline. Future work should include independent validation using total station surveys or physical measurements to further quantify pipeline accuracy.

The 1 mm slicing interval was selected to match the approximate layer thickness of the printed walls, ensuring that each slice captures at least one full deposition layer. Because centroid drift is a spatially smooth quantity governed by gradual printer kinematics rather than layer-scale fluctuations, the resulting imperfection metrics (maximum eccentricity and inclination) are expected to be insensitive to moderate changes in slicing interval. Coarser intervals (e.g., 5 mm or 10 mm) would reduce computational cost with minimal effect on the global drift profile, though very coarse intervals may under-sample local deviations. A formal parameter sensitivity study examining the effect of slicing interval, SOR parameters, and boundary reconstruction method on the derived metrics is recommended as future work.

Limitations of the present study include the small sample size (n = 3 walls from a single printer and facility), which restricts the generalisability of the findings to other printing systems, materials, or environmental conditions. The use of a fixed slicing interval increases computational cost. The workflow also relies on identifying a stable analysis region near the base and top to avoid fixture and termination artefacts; further automation of this step would reduce operator judgement. Future work should expand the dataset across multiple print runs, printers, and environmental conditions to establish statistical bounds on imperfection patterns and explore adaptive slicing or accelerated processing to support near-real-time quality assessment on site.

6 Conclusion

This paper provides a practical scan-to-metrics workflow to quantify initial geometric imperfections in full-scale 3DCP walls using TLS point clouds and to benchmark the measured imperfection profile against Eurocode 2 criteria for isolated slender members. The workflow combines point-cloud preprocessing, millimetre-scale horizontal slicing, cross-section reconstruction, and PCA-based alignment to produce consistent wall-height profiles of cross-sectional area and centroid drift.

Applied to three full-scale wall specimens, the measured inclination and equivalent eccentricity derived from centroid drift remained within the EC2 limits considered in this study. The scan-derived cross-sectional areas also indicated systematic overprinting relative to the nominal CAD area, underscoring the need to complement dimensional conformity checks with centroid-based imperfection metrics that are more directly connected to second-order effects and stability.

Overall, the study demonstrates that TLS data can be converted into code-relevant imperfection descriptors in a repeatable, non-contact manner, supporting objective quality control and measured-geometry structural assessment of 3DCP walls. Future work should validate the workflow on a larger population of printed elements, automate stable-region identification, and integrate scan-derived imperfection profiles into routine acceptance criteria and modelling workflows for 3DCP construction.

Acknowledgements

This research is supported by Singapore National Additive Manufacturing Innovation Cluster (NAMIC) and Woh Hup (Private) Limited (A-8003034-00-00). The authors wish to express their gratitude to Associate Professor Yeoh Ker-Wei, Justin (National University of Singapore) who has graciously lent us the FARO M70 Focus Laser scanner for this research work.

7 References

[1] J. Otto and P. Maiwald, “Classification and automated quality assurance of 3D concrete printed surfaces,” *Autom. Constr.*, vol. 164, p. 105467, Aug. 2024, doi: 10.1016/j.autcon.2024.105467.

[2] J. M. De Araújo, “Comparative study of the simplified methods of Eurocode 2 for second order analysis of slender reinforced concrete columns,” *J. Build. Eng.*, vol. 14, pp. 55–60, Nov. 2017, doi: 10.1016/j.jobe.2017.10.003.

[3] *European Committee For Standardization. Eurocode 2: Design of Concrete Structures – Part 1-1: General Rules and Rules for Buildings. EN 1992-1-1:2004. Brussels, Belgium; 2004.*

[4] D. Zhang, P. Feng, P. Zhou, W. Xu, and G. Ma, “3D printed concrete walls reinforced with flexible FRP textile: Automatic construction, digital rebuilding, and seismic performance,” *Eng. Struct.*, vol. 291, p. 116488, Sep. 2023, doi: 10.1016/j.engstruct.2023.116488.

[5] Z. Zuo *et al.*, “Systematic workflow for digital design and on-site 3D printing of large concrete structures: A case study of a full-size two-story building,” *J. Build. Eng.*, vol. 104, p. 112370, Jun. 2025, doi: 10.1016/j.jobe.2025.112370.

[6] R. Buswell *et al.*, “Geometric quality assurance for 3D concrete printing and hybrid construction manufacturing using a standardised test part for benchmarking capability,” *Cem. Concr. Res.*, vol. 156, p. 106773, Jun. 2022, doi: 10.1016/j.cemconres.2022.106773.

[7] Open3D, “Point cloud outlier removal.” Accessed: Feb. 11, 2026. [Online]. Available: https://www.open3d.org/docs/latest/tutorial/Advanced/pointcloud_outlier_removal.html

[8] N. T. Mahmooda, M. H. Al-Muifraje, S. K. Salih, and T. R. Saeed, “Pattern Recognition of Composite Motions based on EMG Signal via Machine Learning,” *Eng. Technol. J.*, vol. 39, no. 2A, pp. 295–305, Feb. 2021, doi: 10.30684/etj.v39i2A.1743.